neutral lipids and phospholipids in the liver and shortens the life span. *Biochem Biophys Res Commun* 2004;315:575–580.
9. Fujita T, Inoue H, Kitamura T, Sato N, Shimosawa T, Maruyama N. Senescence marker protein-30 (SMP30) rescues cell death by enhancing plasma membrane Ca(2+)-pumping activity in Hep G2 cells. *Biochem Biophys Res Commun* 1998;250:374–380.
10. Junqueira VB, Barros SB, Chan SS, Rodrigues L, Giavarotti L, Abud RL, Deucher GP. Aging and oxidative stress. *Mol Aspects Med* 2004; 25:5–16.
11. MacNee W. Pulmonary and systemic oxidant/antioxidant imbalance in chronic obstructive pulmonary disease. *Proc Am Thorac Soc* 2005;2: 50–60.
12. Rahman I, van Schadewijk AA, Crowther AJ, Hiemstra PS, Stolk J, MacNee W, De Boer WI. 4-Hydroxy-2-nonenal, a specific lipid peroxidation product, is elevated in lungs of patients with chronic obstructive pulmonary disease. *Am J Respir Crit Care Med* 2002;166:490–495.
13. Barreiro E, de la Puente B, Minguella J, Corominas JM, Serrano S, Hussain SN, Gea J. Oxidative stress and respiratory muscle dysfunction in severe chronic obstructive pulmonary disease. *Am J Respir Crit Care Med* 2005;171:1116–1124.
14. Kasagi S, Seyama K, Mori H, Souma S, Sato T, Akiyoshi T, Suganuma H, Fukuchi Y. Tomato juice prevents from developing emphysema induced by chronic exposure to tobacco smoke in senescence-accelerated mouse P1 strain. *Am J Physiol Lung Cell Mol Physiol* 2006;290: 396–404.
15. Thurlbeck WM. The internal surface area of nonemphysematous lungs. *Am Rev Respir Dis* 1967;95:765–773.
16. Eidelman DH, Bellofiore S, Chiche D, Cosio MG, Martin JG. Behavior of morphometric indices in pancreatic elastase-induced emphysema in rats. *Lung* 1990;168:159–169.
17. Teramoto S, Fukuchi Y, Uejima Y, Teramoto K, Oka T, Orimo H. A novel model of senile lung: senescence-accelerated mouse (SAM). *Am J Respir Crit Care Med* 1994;150:238–244.
18. Levine RL, Garland D, Oliver CN, Amici A, Climent I, Lenz AG, Ahn BW, Shaltiel S, Stadtman ER. Determination of carbonyl content in oxidatively modified proteins. *Methods Enzymol* 1990;186:464–478.
19. Levine RL, Williams JA, Stadtman ER, Shacter E. Carbonyl assays for determination of oxidatively modified proteins. *Methods Enzymol* 1994;233:346–357.
20. Nakamura A, Goto S. Analysis of protein carbonyls with 2,4-dinitrophenyl hydrazine and its antibodies by immunoblot in two-dimensional gel electrophoresis. *J Biochem (Tokyo)* 1996;119:768–774.
21. Dalle-Donne I, Giustarini D, Colombo R, Rossi R, Milzani A. Protein carbonylation in human diseases. *Trends Mol Med* 2003;9:169–176.
22. Liu J, Yeo HC, Doniger SJ, Ames BN. Assay of aldehydes from lipid peroxidation: gas chromatography-mass spectrometry compared to thiobarbituric acid. *Anal Biochem* 1997;245:161–166.
23. Erdelmeier I, Gerard-Monnier D, Yadan JC, Chaudiere J. Reactions of N-methyl-2-phenylindole with malondialdehyde and 4-hydroxyalkenals: mechanistic aspects of the colorimetric assay of lipid peroxidation. *Chem Res Toxicol* 1998;11:1184–1194.
24. Cantin AM, North SL, Hubbard RC, Crystal RG. Normal alveolar epithelial lining fluid contains high levels of glutathione. *J Appl Physiol* 1987;63:152–157.
25. Teramoto S, Fukuchi Y, Uejima Y, Teramoto K, Orimo H. Biochemical characteristics of lungs in senescence-accelerated mouse (SAM). *Eur Respir J* 1995;8:450–456.
26. Stadtman ER, Levine RL. Protein oxidation. *Ann N Y Acad Sci* 2000;899: 191–208.
27. Goto S, Nakamura A. Age-associated, oxidatively modified proteins: a critical evaluation. *Age (Omaha)* 1997;20:81–89.
28. Ishigami A, Handa S, Maruyama N, Supakar PC. Nuclear localization of senescence marker protein-30, SMP30, in cultured mouse hepatocytes and its similarity to RNA polymerase. *Biosci Biotechnol Biochem* 2003;67:158–160.
29. Rangasamy T, Cho CY, Thimmulappa RK, Zhen L, Srisuma SS, Kensler TW, Yamamoto M, Petrache I, Tuder RM, Biswal S. Genetic ablation of Nrf2 enhances susceptibility to cigarette smoke-induced emphysema in mice. *J Clin Invest* 2004;114:1248–1259.
30. Rahman I, Smith CA, Lawson MF, Harrison DJ, MacNee W. Induction of gamma-glutamylcysteine synthetase by cigarette smoke is associated with AP-1 in human alveolar epithelial cells. *FEBS Lett* 1996;396: 21–25.
31. Rahman I, Antonicelli F, MacNee W. Molecular mechanism of the regulation of glutathione synthesis by tumor necrosis factor-alpha and dexamethasone in human alveolar epithelial cells. *J Biol Chem* 1999; 274:5088–5096.
32. Rahman I, Smith CA, Antonicelli F, MacNee W. Characterisation of gamma-glutamylcysteine synthetase-heavy subunit promoter: a critical role for AP-1. *FEBS Lett* 1998;427:129–133.
33. Maruyama N, Ishigami A, Kuramoto M, Handa S, Kubo S, Imasawa T, Seyama K, Shimosawa T, Kasahara Y. Senescence marker protein-30 knockout mouse as an aging model. *Ann N Y Acad Sci* 2004;1019:383–387.
34. Ishii K, Tsubaki T, Fujita K, Ishigami A, Maruyama N, Akita M. Immunohistochemical localization of senescence marker protein-30 (SMP30) in the submandibular gland and ultrastructural changes of the granular duct cells in SMP30 knockout mice. *Histol Histopathol* 2005;20:761–768.
35. Bota DA, Davies KJ. Protein degradation in mitochondria: implications for oxidative stress, aging and disease: a novel etiological classification of mitochondrial proteolytic disorders. *Mitochondrion* 2001;1:33–49.
36. Kawakami M, Paul JL, Thurlbeck WM. The effect of age on lung structure in male BALB/cNNia inbred mice. *Am J Anat* 1984;170:1–21.
37. Matulionis DH. Chronic cigarette smoke inhalation and aging in mice: 1. Morphologic and functional lung abnormalities. *Exp Lung Res* 1984; 7:237–256.
38. Suga T, Kurabayashi M, Sando Y, Ohyama Y, Maeno T, Maeno Y, Aizawa H, Matsumura Y, Kuwaki T, Kuro OM, *et al.* Disruption of the klotho gene causes pulmonary emphysema in mice: defect in maintenance of pulmonary integrity during postnatal life. *Am J Respir Cell Mol Biol* 2000;22:26–33.
39. Takeda T, Hosokawa M, Higuchi K, Hosono M, Akiguchi I, Katoh H. A novel murine model of aging, Senescence-Accelerated Mouse (SAM). *Arch Gerontol Geriatr* 1994;19:185–192.
40. Aoshiba K, Yokohori N, Nagai A. Alveolar wall apoptosis causes lung destruction and emphysematous changes. *Am J Respir Cell Mol Biol* 2003;28:555–562.
41. Kasahara Y, Tuder RM, Taraseviciene-Stewart L, Le Cras TD, Abman S, Hirth PK, Waltenberger J, Voelkel NF. Inhibition of VEGF receptors causes lung cell apoptosis and emphysema. *J Clin Invest* 2000;106: 1311–1319.
42. Tuder RM, Petrache I, Elias JA, Voelkel NF, Henson PM. Apoptosis and emphysema: the missing link. *Am J Respir Cell Mol Biol* 2003;28: 551–554.
43. Tuder RM, Zhen L, Cho CY, Taraseviciene-Stewart L, Kasahara Y, Salvemini D, Voelkel NF, Flores SC. Oxidative stress and apoptosis interact and cause emphysema due to vascular endothelial growth factor receptor blockade. *Am J Respir Cell Mol Biol* 2003;29:88–97.
44. Petrache I, Natarajan V, Zhen L, Medler TR, Richter AT, Cho C, Hubbard WC, Berdyshev EV, Tuder RM. Ceramide upregulation causes pulmonary cell apoptosis and emphysema-like disease in mice. *Nat Med* 2005;11:491–498.

Histol Histopathol (2006) 21: 1151-1156

http://www.hh.um.es

Histology and Histopathology

Cellular and Molecular Biology

Accelerated tubular cell senescence in SMP30 knockout mice

W. Yumura[1,2], T. Imasawa[3], S. Suganuma[2], A. Ishigami[1], S. Handa[1], S. Kubo[1], K. Joh[3] and N. Maruyama[1]

[1]Department of Molecular Pathology, Tokyo Metropolitan Institute of Gerontology, Tokyo, [2]Department of Medicine, Kidney Center, Tokyo Women's Medical University, Tokyo, [3]Department of Internal Medicine and Division of Immunopathology, Clinical Research Center, Chiba-East National Hospital, Chiba, Japan.

Summary. An experimental model with accelerated but not drastic renal senescence seemed useful to recognize the mechanisms of how kidney function deteriorates with age. Senescence marker protein-30 (SMP30), whose expression decreased with age and was sex-independent, is mainly expressed in hepatocytes and proximal tubular cells. Therefore, we established a SMP30 deficient strain of mice with a C57BL/6 background by gene targeting to investigate whether this molecule is involved in renal tubular cell senescence. Male SMP30 knockout (SMP30Y/-) mice and male wild-type (SMPY/+) mice (n=5) aged 12 months were examined histologically. Their tubular epithelia showed the deposition of lipofuscin and the presence of senescence-associated ß-galactosidase (SA-ß-GAL). However, no tubular cells were atrophic. In electron microscopy, SMP30-KO mice showed markedly enlarged lysosomes containing an electron dense substance. These are convincing hallmarks of senescence. We recognized the early manifestation of senescence hallmarks in SMP30-KO mice at 12 months old. Thus, this model represents the first report of a mouse strain that manifests accelerated ordinal senescence in a kidney after gene manipulation.

Key words: Renal senescence, Tubular cells, SMP30, Knockout mouse, Lipofuscin, Senescence-associated, ß-galactoside

Offprint requests to: M.D. Ph.D. Toshiyuki Imasawa, Department of Internal Medicine and Division of Immunopathology, Clinical Research Center, Chiba-East National Hospital, 673 Nitona, Chuoh, Chiba, 260-8712, Japan. e-mail: timasawa@yahoo.co.jp. W.Y. and T.I both contributed equally to this work

Introduction

Aging results in profound anatomic and functional deterioration in renal systems both in humans (Davies and Shock, 1950; Hoang et al., 2003; Melk et al., 2004) and in animals (Yumura et al., 1989; Melk et al., 2003). These changes increase the risks for acute renal failure or chronic renal failure. In addition, kidney transplantation from the elderly performed poorly (Moreso et al., 1999; Kasiske and Snyder, 2002). Therefore, much attention has been devoted to studies of aging kidney. Renal senescence is a pleiotropic phenomenon induced by both intrinsic and extrinsic factors. This phenomenon appears gradually but inevitably as every individual ages. Seeking influential factors that induce senescence is a compelling subject.

In contrast, considerable evidence has accumulated of the molecular contribution to senescence in mitotic cells. Cultured mammalian somatic cells, such as fibroblasts, after a finite number of population doublings, eventually reach a state in which they irreversibly cease replication and manifest abnormalities (Hayflick and Moorhead, 1961; Wright and Shay, 2002). This state has been called replicative or cellular senescence. Senescent cells are identified in culture by their failure to synthesize with passage. In vitro, however, cell growth is not easily manipulated or monitored, and measurements of DNA synthesis do not distinguish senescent cells from quiescent or terminally differentiated cells. Dimri et al. reported that senescence-associated b-galactosidase (SA-ß-GAL) could be a good marker of replicative senescence. An age-dependent manifestation of SA-ß-GAL in human skin is the accumulation of senescent fibroblasts and keratinocytes *in vivo* (Dimri et al., 1995). In addition, lipofuscin is, apparently, a universal feature of aging (Harman, 1989).

Numerous molecules are associated with senescence. During a survey of such molecules by proteomic

analysis, we discovered a novel molecule in the rat liver (Fujita et al., 1992). Its expression decreased with age and was sex-independent. We designated this molecule as senescence marker protein-30 (SMP30). Phylogenically, the amino acid sequence of this molecule was highly conserved among all animals examined (not published). However, the function of this molecule is not entirely clear. Subsequently, we established a SMP30 deficient strain of mice with a C57BL/6 background by gene targeting (Ishigami et al., 2002). This strain is very sensitive to apoptosis induced by anti-Fas antibody or TNF-α and the lack or decrease of SMP30 seemed to cause organ frailty with aging. Recently we observed that the life span of SMP30-knockout (KO) mice was shorter than that of the wild type strain (Ishigami et al., 2004). Although SMP30 is expressed in almost all organs, the prominent sites expressing this molecule are the liver and kidney (Fujita et al., 1992, 1999). The proximal region of tubular epithelial cells expresses SMP30 abundantly. Since the deficiency of SMP30 in these KO mice can be regarded as the ultimate decrease, one can expect that they will undergo substantial organ deterioration with aging.

An experimental model with accelerated but not drastic senescence seemed useful not only to recognize the mechanisms of how kidney function deteriorates with age but also to use studies for disease susceptibility of aging kidneys. The desirable animal model in which to study kidney aging is one that manifests hallmarks of senescence at an early stage.

Materials and methods

Animals

The SMP30 knockout mice with C57BL/6 background were generated by gene targeting (Ishigami et al., 2002). In the present study, we used male SMP30 knockout (SMP30Y/-) mice (n=5) and male wild-type (SMP30Y/+) mice (n=5) aged 12 months. Mice were maintained at 12 hours day/dark cycles in a controlled environment and fed ad libitum. The Animal Care and Use Committee of Tokyo Metropolitan Institute of Gerontology approved the protocol of the animal experiment performed in the present study. To obtain renal tissues, mice were exsanguinated via abdominal aorta under anesthesia with intraperitoneal injection of pentobarbital (10 mg per 100 g body weight) and perfused via portal vein with phosphated-buffered saline (PBS).

Histological examination

Paraffin embedded specimens were cut at 2 μm and stained with periodic acid-Schiff for histopathological assessment. For electron microscopy, mouse kidneys were fixed with 2.5% glutaraldehyde in PBS. The specimens were post-fixed in 1% osmium tetroxide, dehydrated in a graded alcohol series, and embedded in epoxy resin. Semi-thin sections (1 μm) were stained with toluidine blue and examined under a light microscope. Then, ultrathin sections were prepared for double staining with urayl acetate and lead citrate; samples were then viewed under a Hitachi 100 electron microscope (Hitachi High-Technologies, Japan).

Senescence-associated (SA) ß-galatosidase (ß-GAL) staining

SA-ß-GAL staining was done by Senescence Detection Kit (BioVision Research Products, Mountain View, CA). The kidney sections embedded in OCT compound were fixed with Fixative solution for 10 minutes at room temperature, and then washed 3 times with PBS. The sections were incubated with Staining Solution Mix overnight at 37°C. Then, the sections were counterstained with hematoxylin and eosin. Positive reaction was detected as a blue color under light microscopy.

Results

Accumulation of lipofuscin in proximal tubular cells was accelerated in SMP30-KO mice

Light microscopically, glomeruli of SMP30-KO mice at 12 months old showed normal appearance comparable to wild type mice. Tubular atrophy, interstitial fibrosis, and atherosclerosis were not observed in all examined mice. The prominent morphological feature of kidneys from SMP30-KO mice was a massive accumulation of lipofuscin (age pigment) in proximal tubular epithelial cells (Fig. 1a,b), and these granules were predominantly observed in S2 or S3 segments. Lipofuscin accumulation in tubular cell was detected in all SMP30-KO mice examined at 12 moths old. However, kidneys from the wild type mice contained little lipofuscin (Fig. 1c,d).

Expression of senescence-associated ß-galactosidase in proximal tubular cells increased in SMP30-KO mice

Another hallmark of senescence is SA-ß-GAL (Morreau et al., 1989; Campisi, 1996). In renal tissues from SMP30-KO mice, SA-ß-GAL staining was observed only in proximal tubular cells, but not in glomeruli or vessels (Fig. 2a,b). However, in wild type no SA-ß-GAL was found (Fig. 2c,d). Although we have noted that lipofuscin is always deposited with SA-ß-GAL, some tubular epithelial cells without detectable lipofuscin deposition were positive for SA-ß-GAL in samples from the SMP30-KO mice.

Enlarged lysosomes were present in tubular cells of SMP30-KO mice

Ultrastructural study of kidneys from SMP30-KO mice showed markedly enlarged lysosomes containing

an electron dense substance in their tubular cells (Fig. 3). On the other hand, lysosomes in tubular cells of wild type appeared normal (not shown).

Discussion

In humans, various types of progeria caused by genetic disorder were reported. The extent of symptoms varies in each progeria. The phenotypes of such disorders usually differ from those of ordinal senescence. Consequently, human progeria has not inspired an appropriate experimental model available by gene manipulation. Some strains of mice having extended life spans or extreme acceleration of senescence have been reported (Kuro-o et al., 1997; Migliaccio et al., 1999), but the mechanisms elucidated by those systems are not always applicable to ordinal senescence. Furthermore, to establish an appropriate experimental model for aging research, some consensus on the criteria of accelerated aging is required. On the basis of previous reports by many investigators, the accelerated deposition of lipofuscin and SA-ß-GAL can

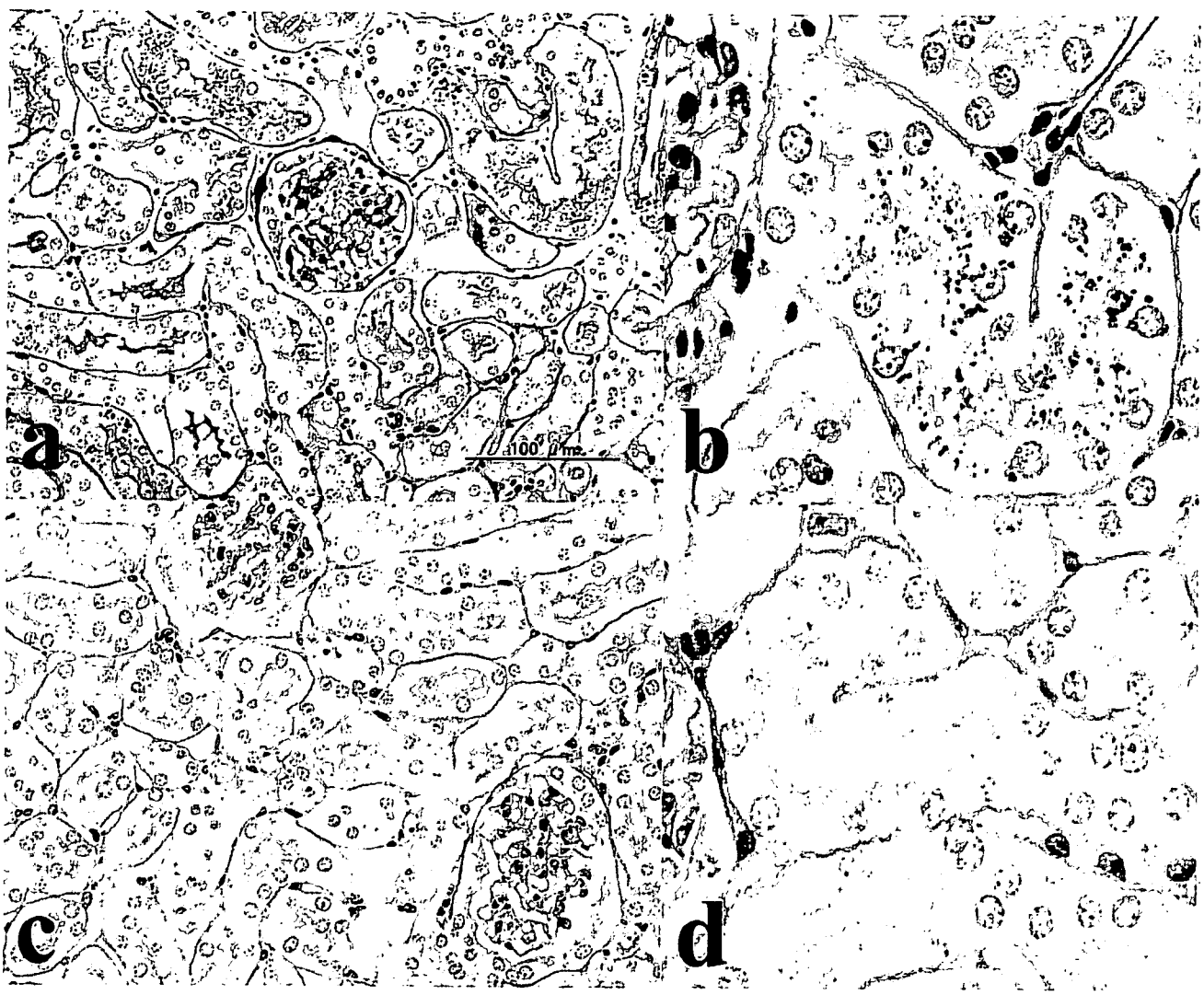

Fig. 1. Lipofuscin deposits accumulate abundantly in renal tubular epithelia of 12-month-old SMP30-KO mice. Paraffin-embedded tissue fixed in 10% formalin were cut at 2 μm and stained with periodic acid-Schiff for histopathological assessment. **a and b.** In the section from a 12-month-old SMP30-KO mouse, numerous brown granules were identified in proximal tubular cells as lipofuscin. **c and d.** In a wild type (SMP30-WT) mouse, kidney section contained very few lipofuscin granules. There were no tubular atrophy, interstitial injuries, and atherosclerosis in either group. Glomeruli also showed normal appearance. a,c x 200; b,d, x 400

serve as an adequate standard for measuring senescence.

In the present study we recognized the early manifestation of both senescence markers in the tubular epithelia of SMP30-KO mice. SMP30-KO mice showed marked deposition of lipofuscin (Fig. 1a,b). In contrast, lipofuscin deposits were barely detectable in comparable wild-type mice (Fig. 1c,d). Melk et al. reported that marked deposition of lipofuscin was present mainly in proximal tubules of aged rats and the largest amounts of lipofuscin lay in atrophic cells (Melk et al., 2003). Although SMP30-KO mice also had tubular cells with lipofuscin, there were no atrophic tubular cells in spite of the lipofuscin accumulation. This indicates that lipofuscin deposition precedes tubular atrophy. Apparently, then, SA-ß-GAL formation precedes lipofuscin deposition in SMP30-KO mice (Fig. 2). Thus the deposition of lipofuscin and SA-ß-GAL expression can be regarded as early parameters of organ senescence in our KO mice. Many reports described that proteinuria induce tubular injury (Chen et al., 1997). However, no albuminuria was detected in all SMP30-KO mice by single radial immunodifusion (data not shown). Therefore, these characteristics of tubular cell in SMP30-KO mice were not associated with proteinuria.

Brunk proposed the mitochondrial-lysosomal axis theory of aging (Brunk and Terman, 2002). According to

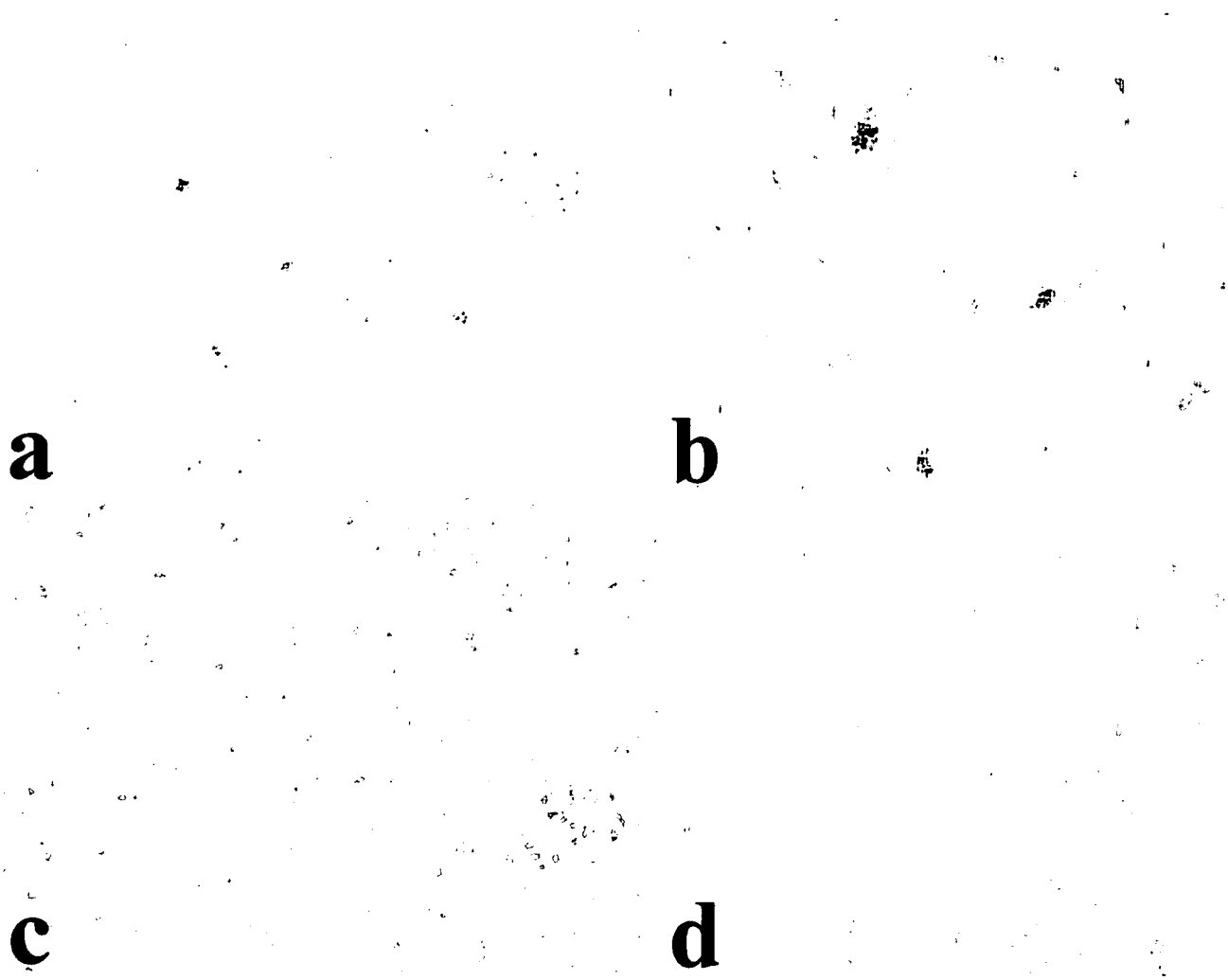

Fig. 2. a and b. SA-ß-GAL staining is positive in kidney tissue from 12-month-old SMP30-KO mice. SA-ß-GAL expression in the kidney section from a 12-month-old SMP30-KO mouse was detected only in proximal tubules, not glomeruli or vessels. **c and d.** Hematoxylin and eosin staining revealed lipofuscin deposition in SA-ß-GAL-positive tubular cells. Tubular cells of a 12-month-old wild type mouse barely expressed SA-ß-GAL. a, c, x 200; b, d x 400

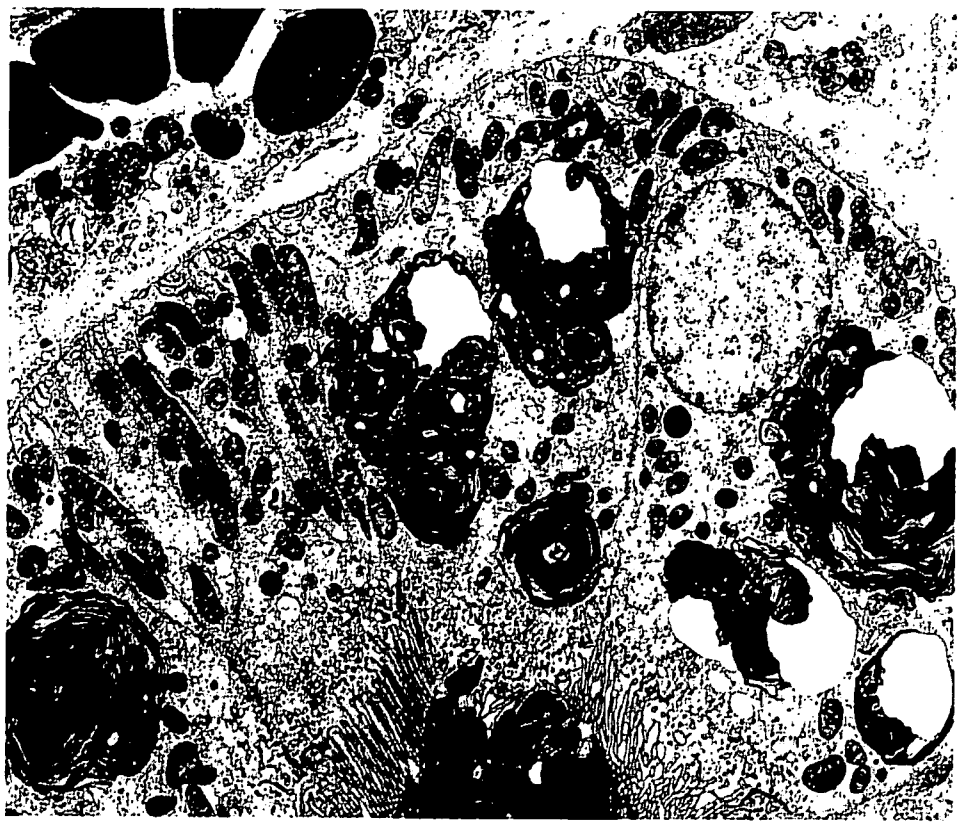

Fig. 3. Ultrastructural analysis revealed greatly enlarged lysosome containing an electron dense substance in a SMP30-KO mouse. x 800

that theory, age-associated accumulations of damaged mitochondria result from imperfect autophagocytosis. We did not observe marked mitochondrial decay in the present study. However, our previous examination of submandibular glands in 12-month-old SMP30-KO mice showed a high proportion of large mitochondria (Ishii et al., 2002). Ultrastructural changes of those membranes ranged from swelling and loss of cristae to complete deterioration and homogenization. Such morphological changes are associated with impaired fission. Additionally, abnormally enlarged mitochondrias are less likely to be autophagocytosed and recycled than those of normal size, leading to further mitochondrial damage. The mitochondrial decay observed in submandibular glands of SMP30-KO might be duplicated in the kidneys of much more aged individuals. We noted pronounced lysosomal enlargement along with extensive lipofuscin deposition in SMP30-KO mice (Fig. 3). Oxidative modification occurs primarily during autophagocytotic degradation inside lysosomes. Lipofuscin seems to undergo maturation reactions and form aggregates that finally may take over whole lysosomes. The process identified here corresponds with the mitochondrial-lysosomal axis theory of aging.

This is the first report of a mouse strain that manifests an acceleration of ordinal senescence after gene manipulation. This strain is expected to have many applications and holds particular promise for locating the missing-link between SMP30 deficiency and hallmarks of senescence.

Acknowledgements. We thank Ms. Phyllis Minick for her excellent editorial assistance and Ms. Tomoko Saito for her secretarial assistance. We also greatly appreciate the technical support given by Hideki Nakayama, Mayuko Oono, and Shigeru Horita. This work is supported by a grant-in-aid for Scientific Research from the Ministry of Education, Science, and Culture, Japan; and a grant from the Health Science Research Grants for Comprehensive Research on Aging and Health supported by Ministry of Health Labor and Welfare, Japan.

References

Brunk U.T. and Terman A. (2002). The mitochondrial-lysosomal axis theory of aging. Accumulation of damaged mitochondria as a result of imperfect autophagocytosis. Eur. J. Biochem. 269, 1996-2002.

Campisi J. (1996). Replicative senescence: an old lives' tale? Cell 84, 497-500.

Chen L., Wang Y., Tay Y.C. and Harris D.C. (1997). Proteinuria and tubulointerstitial injury. Kidney Int. 61, S60-62.

Davies D.F. and Shock N.W. (1950). Age changes in glomerular

filtration rate, effective renal plasma flow, and tubular excretory capacity in adult males. J. Clin. Invest. 29, 496-507.

Dimri G.P., Lee X., Basile G., Acosta M., Scott G., Roskelley C., Medrano E.E., Linskens M., Rubelj I., Pereira-Smith O., Peacocke M. and Campisi J. (1995). A biomarker that identifies senescent human cells in culture and in aging skin in vivo. Proc. Natl. Acad. Sci. USA 92, 9363-9367.

Fujita T., Uchida K. and Maruyama N. (1992). Purification of senescence marker protein-30 (SMP30) and its androgen-independent decrease with age in the rat liver. Biochim. Biophys. Acta 1116, 122-128.

Fujita T., Shirasawa T. and Maruyama N. (1999). Expression and structure of senescence marker protein-30 (SMP30) and its biological significance. Mech. Ageing Dev. 107, 271-280.

Harman D. (1989). Lipofuscin and ceroid formation: the cellular recycling system. Adv. Exp. Med. Biol. 266, 3-15.

Hayflick L. and Moorhead P.S. (1961). The serial cultivation of human diploid cell strains. Exp. Cell. Res. 25, 585-621.

Hoang K., Tan J.C., Derby G., Blouch K.L., Masek M., Ma I., Lemley K.V. and Myers B.D. (2003). Determinants of glomerular hypofiltration in aging humans. Kidney Int. 64, 1417-1424.

Ishigami A., Fujita T., Handa S., Shirasawa T., Koseki H., Kitamura T., Enomoto N., Sato N., Shimosawa T. and Maruyama N. (2002). Senescence marker protein-30 knockout mouse liver is highly susceptible to TNF-α- and Fas-mediated apoptosis. Am. J. Pathol. 161, 1273-1281.

Ishigami A., Kondo Y., Nanba R., Ohsawa T., Handa S., Kubo S., Akita M. and Maruyama N. (2004). Senescence marker protein-30 deficiency in mice causes an accumulation of neutral lipids and phospholipids in the liver and shortens the life span. Biochem. Biophys. Res. Commun. 315, 575-580.

Ishii K., Abe K. and Tsubaki K. (2002). Localization of senescence marker protein-30 (SMP30) in the mouse submandibular gland and histological findings in the SMP30 knock-out mouse. Otolar. Jpn. 105, 915-919.

Kasiske B.L. and Snyder J. (2002). Matching older kidneys with older patients does not improve allograft survival. J. Am. Soc. Nephrol. 13, 1067-72.

Kuro-o, M. Matsumura Y., Aizawa H., Kawaguchi H., Suga T., Utsugi T., Ohyama Y., Kurabayashi M., Kaname, T., Kume E., Iwasaki H., Iida A., Shiraki-Iida T., Nishikawa S., Nagai R. and Nabeshima Y.I. (1997). Mutation of the mouse klotho gene leads to a syndrome resembling aging. Nature 309, 45-51.

Melk A., Kittikowit W., Sandhu I., Halloran K.M., Grimm P., Schmidt B.M. and Halloran P.F. (2003). Cell senescence in rat kidneys in vivo increases with growth and age despite lack of telomere shortening. Kidney Int. 63, 2134-2143.

Melk A., Schmidt B.M., Takeuchi O., Sawitzki B., Rayner D.C. and Halloran P.F. (2004). Expression of $p16^{INK4a}$ and other cell cycle regulator and senescence associated genes in aging human kidney. Kidney Int. 65, 510-520.

Migliaccio E., Giorgio M., Mele S., Pelicci G., Reboldi P., Pandolfi P.P., Lanfrancone L. and Pelicci P.G. (1999). The p66shc adaptor protein controls oxidative stress response and life span in mammals. Nature 402, 309-313.

Moreso F., Seron D., Gil-Vernet S., Riera L., Fulladosa X., Ramos R., Alsina J. and Grinyo J.M. (1999). Donor age and delayed graft function as predictors of renal allograft survival in rejection-free patients. Nephrol. Dial. Transplant. 14, 930-935.

Morreau H., Galjart N.J., Gillemans N., Willemsen R., van der Horst G.T. and d'Azzo A. (1989). Alternative splicing of beta-galactosidase mRNA generates the classic lysosomal enzyme and a beta-galactosidase-related protein. J. Biol. Chem. 264, 20655-20663.

Wright W.E. and Shay J.W. (2002). Historical claims and current interpretations of replicative aging. Nat. Biotechnol. 20, 682-688.

Yumura W., Sugino N., Nagasawa R., Kubo S., Hirokawa K. and Maruyama N. (1989). Age-associated changes in renal glomeruli of mice. Exp. Gerontol. 24, 237-249.

Accepted May 10, 2006

European Journal of Neurology 2007, 14: 1029–1034 doi:10.1111/j.1468-1331.2007.01870.x

Clinical and experimental features of MuSK antibody positive MG in Japan

K. Ohta[a], K. Shigemoto[b], A. Fujinami[c], N. Maruyama[d], T. Konishi[e] and M. Ohta[a,c]

[a]*Clinical Research Center, Utano National Hospital, Kyoto, Japan;* [b]*Department of Preventive Medicine, Faculty of Medicine, Graduate School of Ehime University, Ehime, Japan;* [c]*Department of Medical Biochemistry, Kobe Pharmaceutical University, Kobe, Japan;* [d]*Tokyo Metropolitan Institute of Gerontology, Tokyo, Japan; and* [e]*Department of Neurology, Utano National Hospital, Kyoto, Japan*

Keywords:
clinical features, domain, IgG subclass, muscle specific tyrosine kinase, MuSK antibody, myasthenia gravis, seronegative myasthenia gravis

Received 28 December 2006
Accepted 7 May 2007

We investigated the presence of antibodies (Abs) against muscle-specific tyrosine kinase (MuSK) in Japanese myasthenia gravis (MG) patients. MuSK Abs were found in 23 (27%) of 85 generalized seronegative MG (SNMG) patients but not in any of the ocular MG patients. MuSK Ab-positive patients were characterized as having female dominance (M:F, 5:18), age range at onset 18 to 72 (median 45) years old, and prominent oculobulbar symptoms (100%) with neck (57%) or respiratory (35%) muscle weakness. Limb muscle weakness was comparatively less severe (52%), thymoma absent. Most patients had good responses to simple plasma exchange and steroid therapy. MuSK IgG from all 18 patients was exclusively the IgG 4 subclass and bound mainly with the MuSK Ig 1–2 domain. Serial studies of 12 individuals showed a close correlation between the variation in MuSK Ab titers and MG clinical severity ($P = 0.01$ by Kruskal–Wallis). MuSK Ab titers were sharply decreased in patients who had a good response to early steroid therapy or simple plasma exchange, but there was no change, or a rapid increase on exacerbation after thymectomy. Measurement of MuSK Ab titers aids in the diagnosis of MG and the monitoring of clinical courses after treatment.

Introduction

Muscular weakness in most patients with myasthenia gravis (MG) is caused by an antibody (Ab)-mediated autoimmune response to muscle nicotinic acetylcholine receptors (AChRs), but there is no correlation between the AChR Ab level and degree of muscle weakness. This may be because of AChR Abs heterogeneity and epitope specificity or the presence of Abs against other functionally important muscle antigens. Fifteen percent of patients with generalized MG who have no detectable circulating Abs to AChR are termed seronegative MG (SNMG). Autoantibodies against muscle-specific tyrosine kinase (MuSK) have been identified in that population [1]. The positivity for MuSK Ab in SNMG patients varied from 3.8% to 71% by studies [1–11], which may be due to geographical or ethnic differences. Immunoglobulin allotypes in Caucasian and Chinese MG patients differ from those in Japanese patients [12]. We performed a MuSK Ab survey of a large number of Japanese MG patients and characterized the clinical features of those who were MuSK Ab positive. Furthermore, we investigated the correlation between MuSK Ab titer and disease severity, epitope specificity, and the IgG subclass of MuSK IgG.

Correspondence: Mitsuhiro Ohta, Department of Medical Biochemistry, Kobe Pharmaceutical University, Motoyamakita, Higashinada-ku, Kobe 658–8558, Japan (tel.: +81 78 441 7557; fax: +81 78 441 7559; e-mail: mohta@kobepharma-u.ac.jp).

Patients and methods

Patients

We studied 85 patients (27 men, 58 women, mean age 56 years old, range 18–76 years) who had generalized SNMG and were consistently negative for serum AChR Abs, as well as 272 AChR Ab-positive MG (SPMG) patients (87 men, 185 women, mean age 54 years old; age range 32–74 years); 50 with and 222 without thymoma. The control populations comprised 70 healthy participants (29 men, 41 women; mean age 50 years old, range 27–74 years) and 91 patients (37 men, 54 women; mean age 50 years old, range 32–74 years) with other neurological or immunological diseases (five Lambert-Eaton myasthenic syndrome, six polymyositis, 10 muscular dystrophy, 15 thyroiditis, 10 type 1 diabetes mellitus, five rheumatoid arthritis, 10 multiple sclerosis, five spinal progressive muscular atrophy, five chronic inflammatory demyelinating polyneuropathy, 10 amyotrophic lateral sclerosis, and 10 epilepsy). The study was approved by the ethics committee of Utano National Hospital. All persons gave their informed consent prior to their inclusion in the study.

Preparation of recombinant human MuSK protein

To produce his-tag human MuSK protein, the entire extracellular domain (MuSK 1–4; nucleotides 107–1526,

GenBank/EMBL accession number AF006464) of human MuSK, and MuSK fragments comprised of the first half bearing two Ig-domains (MuSK 1–2; nucleotides 107–700) were linked to the PCR3.1/Myc-His vector (Invitrogen Corporation, Carlsbad, CA, USA) [13]. Membrane-proximal extracellular domains, including Ig-domains 3 and 4 (MuSK 3–4; nucleotides 701–1526), were linked to the pSecTag-His vector (Invitrogen) carrying the ER signal sequence of the mouse Igκ gene. All constructs were transiently transfected to COS7 cells [14]. The recombinant his-tag MuSK secreted was purified in a histidine-affinity column (Clonetech Laboratories, Palo Alto, CA, USA). Recombinant protein purity was determined by SDS-PAGE with silver staining. Recombinant protein concentrations were obtained with a BCA Protein assay kit (Pierce, Biotechnology, Inc., Rockfold, IL, USA) with bovine serum albumin as the standard. The MuSK extracellular domain and MuSK fragments then were labeled with ^{125}I [15].

Detection of MuSK Ab by radioimmunoprecipitation assay

All the sera underwent a radioimmunoassay (RIA) to determine the presence of MuSK Ab. In brief, 5 μl of each sample was incubated overnight at 4°C with 50 μl of ^{125}I-his-tag MuSK (40 000 cpm), after which 50 μl of anti-human IgG was added, and the sample incubated for another 2 h at room temperature. Radioactivity was counted after two washes of the pellets with saline. All positive sera were titrated, and results expressed as nanomoles of ^{125}I-MuSK precipitated per liter of serum.

Epitope mapping

Muscle-specific tyrosine kinase Ab-positive sera were tested by an RIA for the presence of IgG Abs to MuSK 1–2 or MuSK 3–4. In brief, 5 μl of each sample was incubated overnight at 4°C with ^{125}I-his-tag MuSK (40 000 cpm), ^{125}I-his-tag MuSK 1–2 (30 000 cpm), or ^{125}I-his-tag MuSK 3–4 (30 000 cpm), after which 50 μl of anti-human IgG was added. The samples then were incubated for another 2 h at room temperature. Radioactivity was counted after two washes of the pellets with saline.

IgG subclasses of MuSK Ab

Microtiter plates (Breakapart plate, Nunk-Immuno Module, Roskilde, Denmark) were coated with 100 μl of 10 μg/ml of each Ab to IgG subclasses (sheep polyclonal anti-human IgG1, 2, 3 and 4; Binding Site, Birmingham, UK) diluted with 10 mM sodium carbonate-bicarbonate buffer, pH 9.3 and kept for 1 h at room temperature. Nonspecific binding sites were saturated with 200 μl PBS containing 5% skimmed milk and 10% Blockace (Dainippon Seiyaku, Osaka, Japan) for 2 h at room temperature. A serum sample (20 μl), first incubated for 2 h at room temperature with ^{125}I-MuSK (30 000 cpm), was added to a plate, and the whole incubated for 2 h at room temperature. After four washes, ^{125}I was counted in each well.

Statistical analysis

Statistical analysis was performed by regression analysis, Kruskal–Wallis, one-way analysis of variance, and Student *t* test. A *P*-value of <0.05 was considered significant.

Results

MuSK Abs

The cut-off value (0.01 nM) was calculated from the mean + 3SD of the healthy subjects' values obtained by an RIA constructed with ^{125}I-MuSK extracellular domains. MuSK Ab was present in 23 (27%) of the 85 SNMG patients but not in any of the 272 SPMG patients, healthy subjects and patients with other neurological or immunological diseases (Fig. 1). Ab-positive samples were confirmed by serial dilution tests, and titers shown as nanomoles of ^{125}I-MuSK precipitated per liter of serum. MuSK Ab titers ranged from 8.4 to 240 nM (median, 57 nM). All the positive serum samples had extremely high titers on ^{125}I-human MuSK immunoprecipitation.

Clinical features of patients with MuSK Abs

Table 1 shows the clinical features of 23 MuSK Ab-positive patients. MuSK Ab in generalized SNMG showed female predominance (five men, 18 women) but not in ocular MG. Age at onset ranged from 18 to 72 years old (median 45 years). Clinical features of MuSK Ab-positive patients were confined to ocular [ptosis, 13/23 (57%) and double vision, 18/23 (78%)]; bulbar [dysphagia: 23/23 (100%), dysarthria: 19/23 (83%)]; neck extensor, 13/23 (57%); respiratory 8/23 (35%) muscle weaknesses. Prevailing weaknesses affected the oculobulbar and respiratory muscles of MuSK Ab-positive patients. About 48% (11/23) had no limb weakness. No thymomas were detected by CT. Six (26%) of the 23 MuSK Ab-positive patients who were thymectomized, had histological abnormalities including small hyperplastic features.

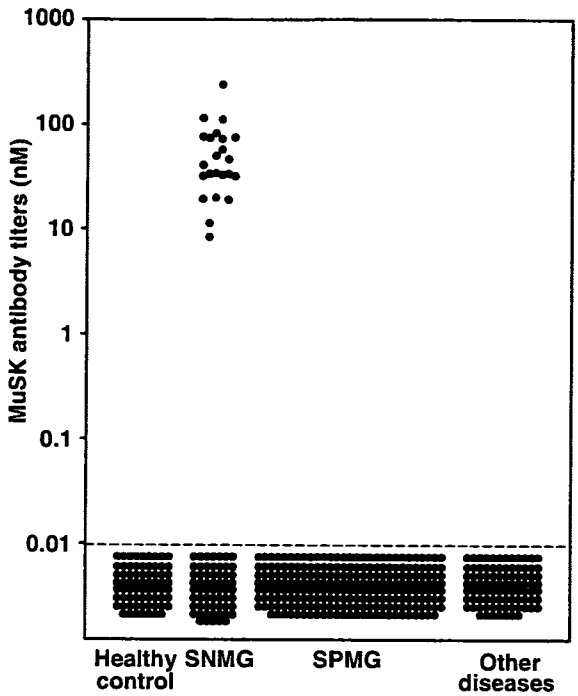

Figure 1 RIA-detected MuSK Ab titers of 85 patients with SNMG, 272 patients with SPMG, 91 patients with other neurological or immunological diseases, and 70 healthy participants. Broken line, the cutoff (0.01 nM) for MuSK Abs.

Table 1 Clinical features of MuSK Ab-positive patients

MuSK Ab positivity in SNMG	23/85 (27%)
MuSK Ab titers	8.4–239 (median 57 nM)
F:M	18:5
Age at onset	18–72 years (median 45 years)
Distribution of weakness	
Ptosis	13/23 (57%)
Ocular motor dysfunction	18/23 (78%)
Bulbar	23/23 (100%)
Neck	13/23 (57%)
Respiratory (crises)	8/23 (35%)
Limb	12/23 (52%)
Thymus	
Thymoma	0/23 (0%)
Hyperplasia	6/23 (26%)

Serial studies of clinical status and MuSK Abs

We measured MuSK Ab titer serially during the disease's course. Table 2 shows anti-MuSK Ab titers in relation to disease severity and duration, and immunosuppressive treatment (A), plasma exchange (B), or thymectomy (C). Disease severity was graded according to the Myasthenia Gravis Foundation of America (MGFA) classification [16] at the onset of myasthenic symptoms, in the maximally deteriorated state, and at

Table 2 Changes in MuSK Ab titers and in clinical status in MuSK Ab-positive patients

Case	Gender	Age at onset (years)	Duration (days)	MuSK Ab (nM)	MGFA classification	treatment
(A) Early steroid therapy						
P-1	F	18	0	39.3	IIIb	
			56	39.0		Pred
			82	40.2		Pred
			138	38.0		Pred
			175	35.0	IIb	Pred
			313	33.0	PR	Pred
			577	21.0		Pred
P-2	F	32	0	113.0	IVb	Pred
			141	17.0		Pred
			261	15.0	IIb	Pred
			409	16.0		Pred
P-3	F	48	0	80.0	IVb	Pred
			46	28.0		Pred
			101	5.0		Pred
			1,641	4.2	PR	Pred
P-4	F	53	0	36.8	IIIb	
			41	31.0		Pred
			97	15.2		Pred
			111	10.0	IIb	Pred
P-5	F	52	0	240.0	V	Pred
			49	57.0		Pred
			77	22.9		Pred
			101	8.4		Pred
			129	3.0	IIb	Pred
P-6	F	76	0	33.0	IIb	Pred
			83	0.5		Pred
			118	0.2	PR	Pred
(B) Simple plasma exchange (PE)						
P-7	M	53	0	74.4	V	
			42	59.0		
			52	47.0		
			PE ⟶			
			62	28.5	IIb	
			PE ⟶			
			67	17.2		
			125	16.0		Pred
			132	11.5		Pred
			138	9.0	IIb	Pred
P-8	M	71	0	113.9	IVb	
			PE ⟶			
			11	32.1		
			45	32.0		Pred
			219	31.0		Pred
			616	28.0	IIb	Pred
P-9	F	66	0	30.0	IIIb	
			45	40.5		
			361	32.0		
			PE ⟶			
			374	14.0	IIb	
			379	21.2		
			389	29.9		
			403	35.5	IIIb	Pred, Cyclo
			441	25.0		Pred, Cyclo
			476	20.5	IIb	Pred, Cyclo

Table 2 (Continued)

(C) Thymectomy (Tx)						
P-10	F	47	0	20.0		
			47	26.0	IIb	
			Tx ——→			
			95	47.2	IIIb	Pred
			270	19.8	IIb	Pred
P-11	F	52	0	22.6	IIb	
			58	23.2		
			Tx ——→			
			170	21.1		Pred
			255	25.0	IIb	
P-12	F	48	0	16.5	IIb	
			95	17.6		
			Tx ——→			
			210	15.7		Pred
			274	17.0	IIb	

PR, Pharmacological Remission; Pred, Predonisolone; Cyclo, Cyclosporine.

the last clinic visit after or during treatment. As shown in Table 2a, six patients (P1–P6) who underwent early steroid therapy showed impressive clinical improvement associated with a sharp decrease in anti-MuSK Ab titer; from 39.3 to 21.0 nM (P-1), 113.0 to 16.0 nM (P-2), 80.0 to 4.2 nM (P-3), 36.8 to 10.0 nM (P-4), 240.0 to 3.0 nM (P-5), and 33.0 to 0.2 nM (P-6). MG severities showed clinical improvement from class IIIb to pharmacological remission (PR) (P-1), class IVb to IIb (P-2), class IVb to PR (P-3), class IIIb to IIb (P-4), class V to IIb (P-5), and class IIb to PR (P-6).

Muscle-specific tyrosine kinase Ab titers of three patients were measured in serial samples taken before and after simple plasma exchange (Table 2b). The patients responded dramatically to that therapy, Ab titers decreasing from 74.4 to 9.0 nM (P-7), 113.9 to 28.0 nM (P-8), and from 30.0 to 20.5 nM (P-9), indicative of clinical improvement from class V to IIb (P-7), class IVb to IIb (P-8), and class IIIb to IIb (P-9). Moreover, conventional immunosuppression maintained the clinical improvement initially achieved by plasma exchange. In one patient (P-9), the effect had tapered off 45 days after plasma exchange, and Ab titer and disease severity returned to the level before treatment. Prednisolone and cyclosporin administered after MG relapse resulted in slower improvement.

Three patients who had histological abnormalities, including a small hyperplastic thymus, underwent thymectomies (Table 2c). After surgery one patient (P-10) immediately had worsening of dysphagia from class IIb to IIIb associated with a rapid increase in MuSK Ab titer from 26.0 to 47.2 nM. Thymectomy was not effective for the other two patients (P-11, P-12) who showed no change in disease severity and MuSK Ab titer.

We analyzed MuSK Ab titers in relation to quantitative clinical scores on the MGFA scale in serial studies of 12 individuals. MuSK Ab titers and disease severity were correlated ($P = 0.01$ by Kruskal–Wallis).

Epitopes in the extracellular domains of human MuSK

Eighteen sera with MuSK Abs were examined for ^{125}I-MuSK 1–2 and ^{125}I-MuSK 3–4 binding. All predominantly bound to ^{125}I-MuSK 1–2, range 68–97%. Only five of the 18 sera also showed slight binding (20–30%) to ^{125}I-MuSK 3–4 (Table 3).

IgG subclasses of MuSK Abs

In a solid phase RIA with sheep polyclonal antibodies to human IgG subclasses, in all the 18 sera tested MuSK Abs were exclusively IgG4 (Table 4).

Discussion

The MuSK Ab-positive rate found for generalized SNMG patients in Japan was 27% with female predominance (M:F = 5:18). This rate is lower than the 70% positivity originally reported [1] and the 40–50% recently reported [2–7]. It is consistent with the 27–33% reported for Japanese and Korean population [8–10] but significantly higher than the 3.8% Chinese positivity rate [11]. Age at onset ranged from 18 to 72 years old (median, 45 years); 61% of the patients presenting at >40 years of age, later than for Caucasians, and 57–71% of patients presenting at <40 years of age, but the differences was not significant [3,7,17,18].

Table 3 Ratio of MuSK Ig 1–2 and 3–4 Ab in MuSK 1–4 Ab titers

Case	MuSK Ab (nM)	Ig 1–2 domain (%)	Ig 3–4 domain(%)
1	8.4	97.1	2.9
2	19.3	68.1	31.9
3	32.5	81.2	18.8
4	50.0	82.7	17.3
5	33.4	97.3	2.7
6	31.8	95.7	4.3
7	19.9	91.0	9.0
8	11.4	95.2	4.8
9	40.7	87.9	12.1
10	32.0	91.0	9.0
11	33.6	95.0	5.0
12	74.7	95.4	4.6
13	72.0	76.2	23.8
14	46.2	80.8	19.2
15	74.7	96.9	3.1
16	82.2	74.2	25.8
17	110.7	89.5	10.5
18	114.6	71.2	28.8

Table 4 Ratio of IgG subclasses of MuSK Abs

Case	MuSK Ab (nM)	IgG 1 (%)	IgG 2 (%)	IgG 3 (%)	IgG 4 (%)
1	114.6	0.0	0.0	0.0	100.0
2	110.7	0.0	0.0	4.9	95.1
3	82.2	0.0	0.0	0.0	100.0
4	74.7	11.0	21.0	19.0	49.0
5	74.0	4.1	5.0	5.6	85.3
6	72.0	0.0	1.0	0.0	99.0
7	46.2	0.0	0.0	0.0	100.0
8	40.7	5.3	0.0	7.1	87.6
9	33.6	15.1	15.7	0.0	69.2
10	33.4	0.0	0.0	0.0	100.0
11	32.5	5.3	0.0	0.0	94.7
12	32.0	4.2	2.6	1.2	92.0
13	31.8	6.7	6.7	8.3	78.3
14	19.9	0.0	0.0	1.7	98.3
15	19.5	0.0	0.0	0.0	100.0
16	19.3	0.0	0.0	0.0	100.0
17	11.4	0.0	28.9	26.1	45.0
18	8.4	0.0	0.0	0.0	100.0

All the Ab-positive patients had similar patterns of muscle weakness, with prevalent involvement of the bulbar muscles in 100%, ocular symptoms (blepharoptosis and/or double vision) in 80%, and of the respiratory muscles in 35% with frequent myasthenic crises. Limb muscle involvement was comparatively less severe and inconsistent. Japanese MuSK Ab-positive patients therefore have clinical features similar in terms of the predominance of bulbar involvement to those reported for Caucasians.

We evaluated the correlation between MuSK Ab titers and disease severity. Table 2 shows patients who had a good response to early immunosuppressive therapy or simple plasma exchange. Their MuSK Ab titers sharply decreased in parallel with clinical improvement, whereas their Ab titers remained positive. We evaluated the effect of thymectomy in three individuals by measuring MuSK Ab titers in serum samples taken pre- and post-thymectomy. One patient's condition deteriorated after thymectomy and her Ab titer greatly increased. The two others showed neither progression nor Ab titer change during the observation period. Thymectomy therefore did not produce good results. Histological changes in the thymus of MuSK Ab-positive subjects are reported to be minimal and to include rare small germinal centers [19,20] in contrast to SPMG patients who had lymph node-type infiltrates. These findings, together with the lack of benefit of thymectomy, are evidence against a role for the thymus in antigen presentation and antibody production.

Serial studies showed a statistically close correlation between MuSK Ab titers and disease severity. MuSK Ab titers also recently were found to correlate with MG severity [21]. MuSK Ab titers were extremely high in all the positive cases (Fig. 1). The close relationship between clinical status and MuSK Ab, found by monitoring Ab titers, suggests that MuSK Ab has a significant pathogenic role in MG patients. Circulating MuSK Abs, however, are reported not to cause a MuSK or AChR deficiency at the endplates [22]. Recent experimental models (rabbits [13] and mice [23]), developed by immunization with recombinant MuSK ectodomain protein, produced MG-like muscle weakness with reduced AChR clustering at neuromuscular junctions. These findings clarified the pathogenic MG mechanisms produced by MuSK Ab.

The paramount MuSK Ab IgG subclass in our eighteen patients was IgG4. Limb and intercostal muscle biopsies found neither reduction in AChR numbers nor complement deposition [9,24]. The absence of complement deposits at a patient's end plates is explained by the fact that MuSK Ab is mainly IgG class 4 which does not fix complement [5,25]. The MuSK extracellular domain consists of four MuSK immunoglobulin-like (Ig) domains. Binding analysis of MuSK Abs to ^{125}I-MuSK Ig 1–2 or ^{125}I-MuSK Ig 3–4 showed that the eighteen sera tested predominantly bound to the ^{125}I-MuSK Ig 1–2 domain. The epitope was the N-terminal of the extracellular domain of human MuSK as described previously [5]. Furthermore, MuSK Abs have been shown to inhibit agrin-induced clustering of AChRs [26]. In fact, MuSK Ig 1–2 domains are more responsible for agrin responsiveness of MuSK, in contrast to Ig 3-4 domains which are more responsible for rapsyn association. We postulate that this is relevant to our findings of predominant binding analysis to MuSK Ig 1–2. The characteristics of the MuSK IgG subclass and Ab binding epitope in Japanese patients therefore are similar to those of Caucasians.

Muscle-specific tyrosine kinase Ab-positive patients often suffer facial and tongue muscle atrophy [3,27]. Benveniste *et al.*[28] reported that MuSK Ab plasma may affect the expression of atrophy-related protein and that a facial muscle, the masseter, is the most susceptible. Amongst our MuSK Ab-positive patients, four patients had detectable tongue atrophy from a relatively early phase of illness; weakness was moderate in 2 patients and mild in two patients. More *in vitro* and *in vivo* studies are needed to clarify the pathologic mechanisms that cause the muscle weakness produced by MuSK Ab. MuSK Ab detection provides a valuable biological means of support for the clinical diagnosis of MG and a way to monitor its clinical course.

Acknowledgements

This study was supported in part by a grant-in-aid from the Ministry of Education, Culture, Sports, Science and

Technology, Japan, and grants from the High-Tech Research Center, the Kobe Pharmaceutical University Collaboration Fund, and the Science Research Promotion Fund of the Japan Private School Promotion Foundation.

References

1. Hoch W, McConville J, Helms S, Newsom-Davis J, Melms A, Vincent A. Auto-antibodies to the receptor tyrosine kinase MuSK in patients with myasthenia gravis without acetylcholine receptor antibodies. *Nature Medicine* 2001; **7:** 365–368.
2. Vincent A, Bowen J, Newsom-Davis J, McConville J. Seronegative generalized myasthenia gravis: clinical features, antibodies, and their targets. *Lancet Neurology* 2003; **2:** 99–106.
3. Evoli A, Tonali PA, Padua L, *et al.* Clinical correlates with anti-MuSK antibodies in generalized seronegative myasthenia gravis. *Brain* 2003; **126:** 2304–2311.
4. Sanders DB, EI-Salem K, Massey, JM, McConville J, Vincent A. Clinical aspects of MuSK antibody positive-seronegative MG. *Neurology* 2003; **60:** 1978–1980.
5. McConville J, Farrugia ME, Beeson D, *et al.* Detection and characterization of MuSK antibodies in seronegative Myasthenia gravis. *Annals of Neurology* 2004; **55:** 580–584.
6. Zhou L, McConville J, Chaudhry V, *et al.* Clinical comparison of muscle-specific tyrosine kinase (MuSK) antibody-positive and - negative myasthenic patients. *Muscle and Nerve* 2004; **30:** 55–60.
7. Padua L, Tonali P, Aprile I, *et al.* Seronegative myasthenia gravis: comparison of neurophysiological picture in MuSK+ and MuSK- patients. *European Journal of Neurology* 2006; **13:** 273–276.
8. Ohta K, Shigemoto K, Kubo S, *et al.* MuSK Ab described in seropositive MG sera found to be Ab to alkaline phosphatase. *Neurology* 2005; **65:** 1988.
9. Shiraishi H, Yoshimura T, Fukudome T, *et al.* Acetylcholine receptors loss and postsynaptic damage in MuSK antibody-positive myasthenia gravis. *Annals of Neurology* 2005; **57:** 289–293.
10. Lee JY, Sung JJ, Cho JY, *et al.* MuSK antibody-positive, seronegative myasthenia gravis in Korea. *Journal of Clinical Neuroscience* 2006; **13:** 353–355.
11. Yeh JH, Chen WH, Chiu HC, Vincent A. Low frequency of MuSK antibody in generalized seronegative myasthenia gravis among Chinese. *Neurology* 2004; **62:** 2131.
12. Chiu HC, de Lange GG, Willcox N, *et al.* Immunoglobulin allotypes in Caucasian and Chinese myasthenia gravis: differences from Japanese patients. *Journal of Neurology, Neurosurgery, and Psychiatry* 1988; **51:** 214–217.
13. Shigemoto K, Kubo S, Maruyama N, *et al.* Induction of myasthenia by immunization against muscle-specific kinase. *Journal of Clinical Investigation* 2006; **116:** 1016–1024.
14. Hopf C, Hoch W. Tyrosine phosphorylation of the muscle-specific kinase is exclusively induced by acetylcholine receptor-aggregation agrin fragments. *European Journal of Biochemistry* 1998; **253:** 382–389.
15. Hunter WM, Greenwood FC. Preparation of iodine-131 labeled human growth hormone of high specific activity. *Nature* 1962; **194:** 495–496.
16. Jaretzki A, Barohn RJ, Ernstoff RM, Kaminski HJ, Keesey JC, Penn AS. Myasthenia gravis: recommendations for clinical research standards. Task Force of the Medical Scientific Advisory Board of the Myasthenia Gravis Foundation of America. *Neurology* 2000; **55:** 16–23.
17. Lavrnic D, Losen M, Vujic A, *et al.* The features of myasthenia gravis with autoantibodies to MuSK. *Journal of Neurology, Neurosurgery, and Psychiatry* 2005; **76:** 1099–1102.
18. Diaz-Manera JA, Juarez C. Rojas-Garcia R, *et al.* Seronegative myasthenia gravis and antiMuSK positive antibodies: description of Spanish series. *Medicina Clinica (Barc)* 2005; **125:** 100–102.
19. Lauriola L, Ranelletti F, Maggiano N, *et al.* Thymus changes in anti-MuSK-positive and –negative myasthenia gravis. *Neurology* 2005; **64:** 536–538.
20. Leite MI, Strobel P, Jones M, *et al.* Fewer thymic changes in MuSK antibody-positive than in Musk antibody-negative MG. *Annals of Neurology* 2005; **57:** 444–448.
21. Bartoccioni E, Scuderi F, Minicuci GM, *et al.* Anti-Musk antibodies: correlation with myasthenia gravis severity. *Neurology* 2006; **67:** 505–507.
22. Selcen D, Fukuda T, Shen XM, Engel AG. Are MuSK antibodies the primary cause of myasthenic symptoms? *Neurology* 2004; **62:** 1945–1950.
23. Jha S, Xu K, Maruta T, *et al.* Myasthenia gravis induced in mice by immunization with the recombinant extracellular domain of rat muscle-specific kinase (MuSK). *Journal of Neuroimmunology* 2006; **175:** 107–117.
24. Vincent A, Leite MI. Neuromuscular junction autoimmune disease: muscle-specific kinase antibodies and treatments for myasthenia gravis. *Current Opinion in Neurology* 2005; **18:** 519–525.
25. Vincent A, Bowen J, Newsom-Davis J, McConville J. Seronegative generalized myasthenia gravis: clinical features and their targets. *Lancet Neurology* 2003; **2:** 99–106.
26. Farrugia ME, Bonifati DM, Clover L, Cossins J, Beeson D, Vincent A. Effect of sera from AChR-antibody negative myasthenia gravis patients on AChR and MuSK in cell cultures. *Journal of Neuroimmunology*, 2007; **185:** 136–144.
27. Farrugia ME, Robson MD, Clover L, *et al.* MRI and clinical studies of facial and bulbar muscle involvement in MuSK antibody-associated myasthenia gravis. *Brain* 2006; **129:** 1481–1492.
28. Benveniste O, Jacobson L, Farrugia ME, Clover L, Vincent A. MuSK antibody-positive myasthenia gravis plasma modifies MURF-1 expression in C2C12 cultures and mouse muscle in vivo. *Journal of Neuroimmunology* 2005; **170:** 41–48.

Geriatr Gerontol Int 2007; 7: 316–325

REVIEW ARTICLE

Significance of SMP30 in gerontology

Akihito Ishigami and Naoki Maruyama

Aging Regulation, Tokyo Metropolitan Institute of Gerontology, Tokyo, Japan

The expression of senescence marker protein-30 (SMP30) was discovered by proteomic analysis. The fact that this molecule's structure is so highly conserved among numerous species strongly suggests that the age-dependent decrease of SMP30 may contribute to senescence. Research that targeted the *SMP30* gene showed deterioration in several organs accompanied by a shortened life span. We then identified SMP30 as gluconolactonase (GNL). The lactonase reaction with L-gulono-γ-lactone is the penultimate step in vitamin C (L-ascorbic acid) biosynthesis. Our discovery has opened the door to a new aspect of aging studies.

Keywords: aging model, apoptosis, calorie restriction, gluconolactonase, SMP30, vitamin C.

Introduction

Senescence processes are time-dependent, deteriorative and functional changes in all living bodies. After middle age, we humans daily experience loss functions of several organs. However, the degree of deterioration varies in each individual. This variation suggests that senescence is pleiotropic, attributable to numerous candidate molecules. Therefore, to evaluate the extent of senescence, a convenient marker is an absolute requirement. Some modified substances such as 8-oxo-7,8-dihydro-2′-deoxyguanosine (8-oxodG) or a hormone like DHEA-S have been reported as useful for this purpose.[1,2] However, these markers are not directly encoded by the genome. Furthermore, these substances are disadvantageous for modifying a gene to establish a model of aging. Recent advances in gene technology have now provided several useful mouse strains for aging research. In Japan, some well-known aging-prone murine strains (i.e. senescence-accelerated mouse, klotho mice) are presently available.[3,4] Although experiments with those strains have revealed useful data about senescence, they do not cover the whole spectrum in aging research. In this review, we introduce the molecules now considered critical for advancing this area of research and a widely applicable strain of mice.

Accepted for publication 22 April 2007.

Correspondence: Dr Akihito Ishigami PhD, Aging Regulation, Tokyo Metropolitan Institute of Gerontology, 35-2 Sakae-cho, Itabashi-ku, Tokyo 173-0015, Japan. Email: ishigami@tmig.or.jp

Discovery of senescence marker protein-30

In 1991, to search for the molecular abnormality at work in the aging process, we surveyed age-associated changes in soluble proteins from rat livers by using proteomic analysis and two-dimensional gel electrophoresis (2D-PAGE). Thereby, we detected and isolated a novel rat liver protein, which as first calculated had a molecular weight of 30 kDa according to the commercial molecular weight markers then available. Because the amounts of this protein decreased androgen-independently with aging, we named it senescence marker protein-30 (SMP30).[5] That designation of SMP30 was accurate until, in more sensitive resolutions, the mass of a SMP molecule proved to be 34 kDa (Fig. 1). However, the earlier name remained in use.

The next step was to prepare an antiserum to SMP30, which was applied to localize SMP30 and identified this protein most prominently in the liver and kidneys among the various organs tested (Fig. 2).[6] Subsequently, we isolated and characterized two cDNA clones encoding rat SMP30.[7] The open reading frame consisting of 897 bp encoded 299 amino acids. The estimated molecular weight and pI of the deduced polypeptide were 33 387 and 5.1, respectively. Genomic Southern hybridization analysis demonstrated that SMP30 was

 doi: 10.1111/j.1447-0594.2007.00420.x

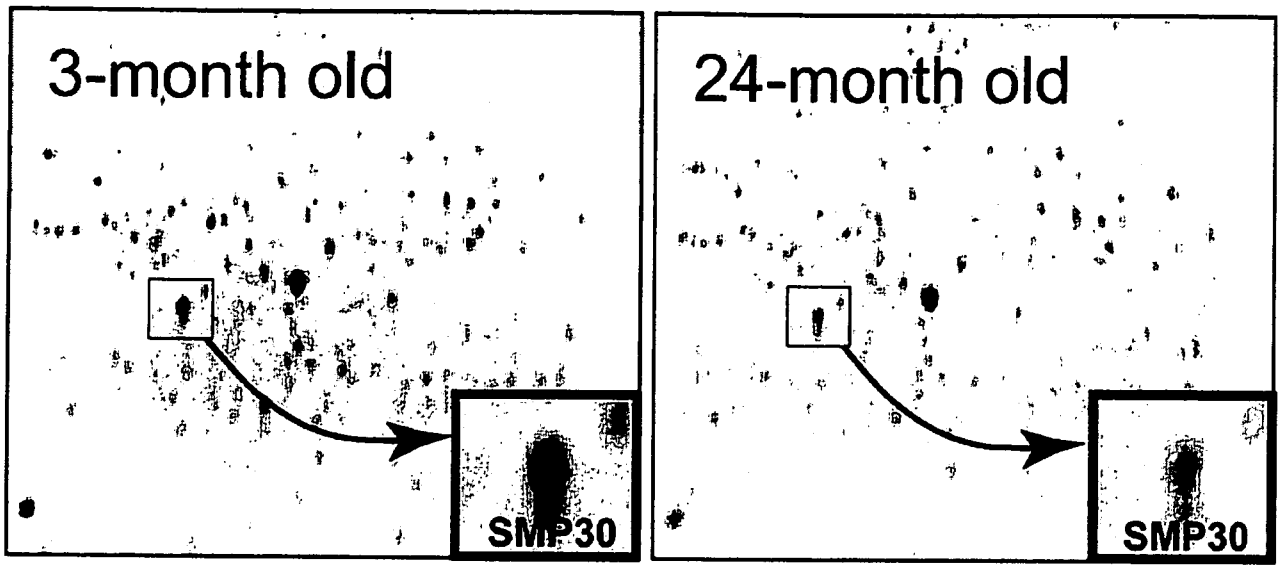

Figure 1 Proteomic profile of senescence marker protein-30 (SMP30) in soluble proteins from 3- and 24-month-old rats. SMP30 is identified as a molecule mass of 34 kDa. Amounts of this protein decrease with aging in an androgen-independent manner.

widely conserved among higher animals. At that time, a computer-assisted homology analysis of nucleic acid and protein databases revealed no marked homology with other known proteins. Therefore, SMP30 seemed to be a novel protein. Additionally, we cloned human SMP30 and documented its 88.6% homology with rat SMP30.[8] The results of regional mapping using a panel of 11 rodent–human somatic hybrids indicated that the gene is located in the p11.3–q11.2 segment of the X chromosome.[8] Analysis of the murine genomic clone revealed that the *SMP30* gene was organized into seven exons and six introns, spanning approximately 17.5 kb[9] Again, the accumulated genomic information showed that the *SMP30* gene is highly conserved among numerous animal species, and this finding was expanded to include non-vertebrates.[10,11] These results indicate the critical biological functions of SMP30.

Functions of SMP30

At the time we discovered SMP30, no functional domain was recognized in the entire amino acid sequence. Subsequently, another research group reported a calcium-binding protein identified with SMP30. However, our purified rat SMP30 and the *Sarcophaga* homolog (anterior fat protein, AFP) failed to show calcium-binding activity.[11,12]

In our laboratory, the evaluation of SMP30 continued for the purpose of examining its possible function in calcium homeostasis.[13,14] Our results established that HepG2 (HepG2/SMP30), a human hepatoma cell line, expressed large amounts of SMP30 after transfection with human cDNA. An investigation followed of the cytosolic free Ca^{2+} concentration ($[Ca^{2+}]i$) and the Na^{+}-independent Ca^{2+} efflux from these cells after extracellular adenosine triphosphate (ATP) stimulation. Although stimulation with ATP caused a transient increase of $[Ca^{2+}]i$ in both HepG2/SMP30 and mock-transfected HepG2 cells, the rate of $(Ca^{2+})i$ decrease after that peak was enhanced twofold by transfection with human SMP30 cDNA. Correspondingly, Ca^{2+} efflux was significantly increased in transfected HepG2/SMP30 cells compared with mock transfectants. In addition, more SMP30 transfectants survived than mock transfectants when cell death was induced by Ca^{2+} ionophore treatment. These results suggested that SMP30 regulates $(Ca^{2+})i$ by modulating the Ca^{2+}-pumping activity on plasma membranes. Therefore, downregulation of SMP30 during aging may contribute to the deterioration of cellular functions.

In 1999, a report on the function of SMP30 appeared in which Billecke *et al.* characterized a novel soluble protein from the mouse liver as having enzymic activity; that is, hydrolysis of diisopropyl phosphorofluoridate (DFP).[15] This molecule also hydrolyzes sarin, soman and tabun, the poisons famously used by Japanese terrorists. However, it lacks paraoxonase and arylesterase activities with respect to paraoxon and phenyl acetate, respectively. Subsequent amino acid sequencing of the purified DFPase showed it to be identical with SMP30.[16] Thus, SMP30 was classified as an enzyme. However, the substrates used in those studies were artificial chemicals developed after World War I.

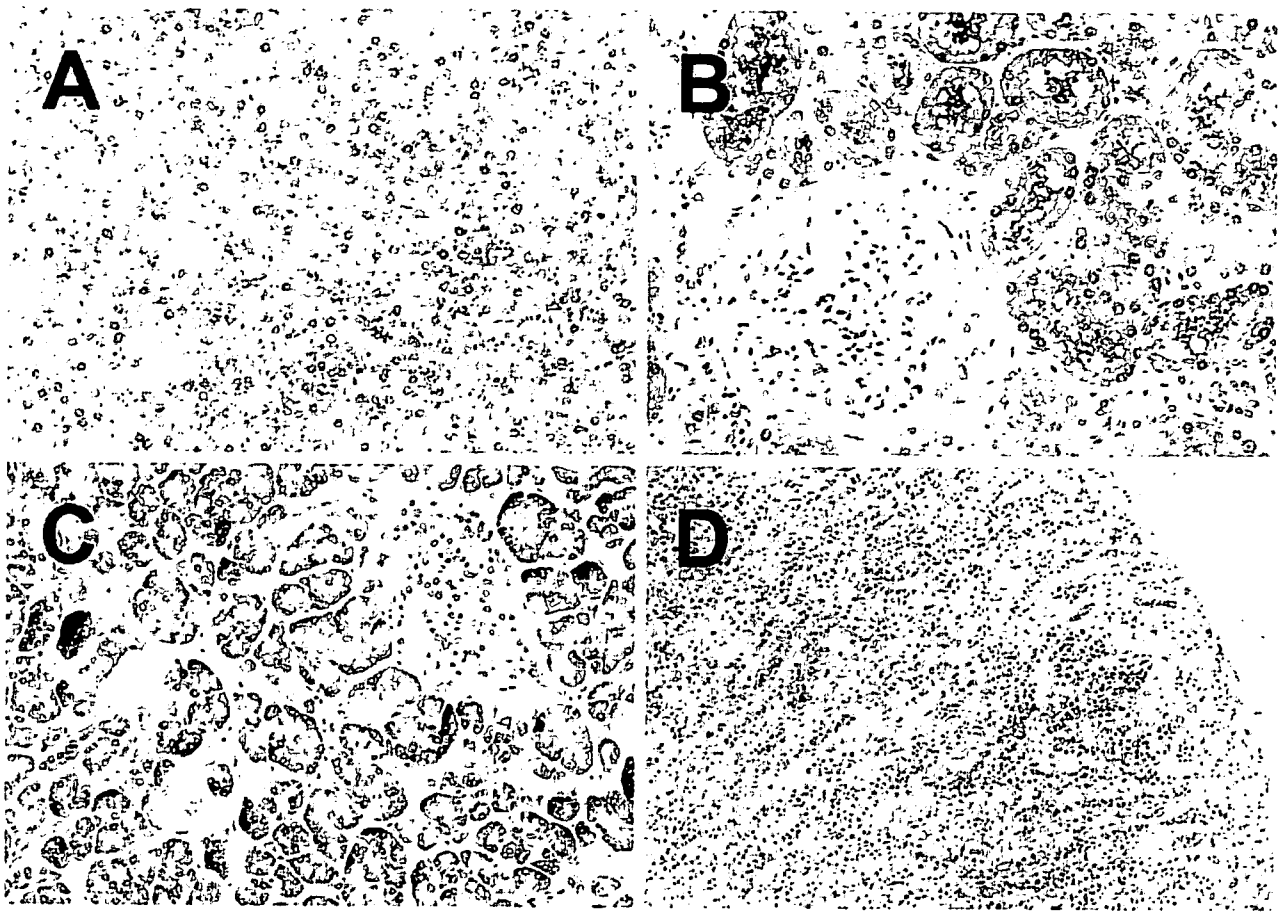

Figure 2 SMP30 expression in human organs. (a) Liver; SMP30 is expressed in parenchymal cells. (b) Kidney; SMP30 is abundant in proximal tubular cells. Localization of SMP30 at the brush border is prominent. (c) Pancreatic; acinal and ductal cells are positive for SMP30. No positive staining occurs in islets of Langerhans. (d) Adrenals; SMP30 is markedly expressed in fasciculata cells of the adrenal cortex.

We also characterized the nature of SMP30 as an organophosphatase.[12] Despite the sequence similarity between SMP30 and a serum paraoxonase (PON), the inability of SMP30 to hydrolyze PON-specific substrates such as paraoxon, dihydrocoumarin, γ-nonalactone and δ-dodecanolactone indicate that SMP30 is distinct from the PON family. The livers from normal mice contained readily detectable DFPase activity, whereas no such enzyme activity was found in livers from mice lacking SMP30. Moreover, the hepatocytes of mice lacking SMP30 were far more susceptible to DFP-induced cytotoxicity than those from the normal mice. This phenomenon accounts for the functional decrease of detoxification in elderly people.

The first report of a natural substrate for SMP30 came from Gomi *et al.*, who identified a SMP30 homolog designated as the luciferin-regeneration enzyme (LRE) in fireflies (*Photius pyralis*).[17,18] LRE converts oxyluciferin to luciferin via an intermediary substance. The deduced amino acid sequence based on cDNA analysis showed at most a 39% identity with insect AFP and mammalian SMP30. However, only 1% of LRE is expressed in the lanterns of fireflies. Despite this possible link to LRE, no genuine function of SMP30 in the whole body has yet been clarified.

Recently, we found a homology between rat SMP30 and two kinds of bacterial gluconolactonase (GNL: EC 3.1.1.17) derived from *Nostoc punctiforme* and *Zymomonas mobilis*.[19] Through subsequent biochemical study, we identified SMP30 as the lactone-hydrolyzing enzyme GNL of animal species.[20] SMP30 purified from the rat liver had lactonase activity toward the aldonolactones D- and L-glucono-δ-lactone, D- and L-gulono-γ-lactone, and D- and L-galactono-γ-lactone, with a requirement for Zn^{2+} or Mn^{2+} as a cofactor. Furthermore, in SMP30-knockout mice, no GNL activity was detectable in the liver. Thus, we concluded that SMP30 is a unique GNL in the liver. In the first report on the discovery of GNL in higher animal species, its molecules were not described in detail.[21]

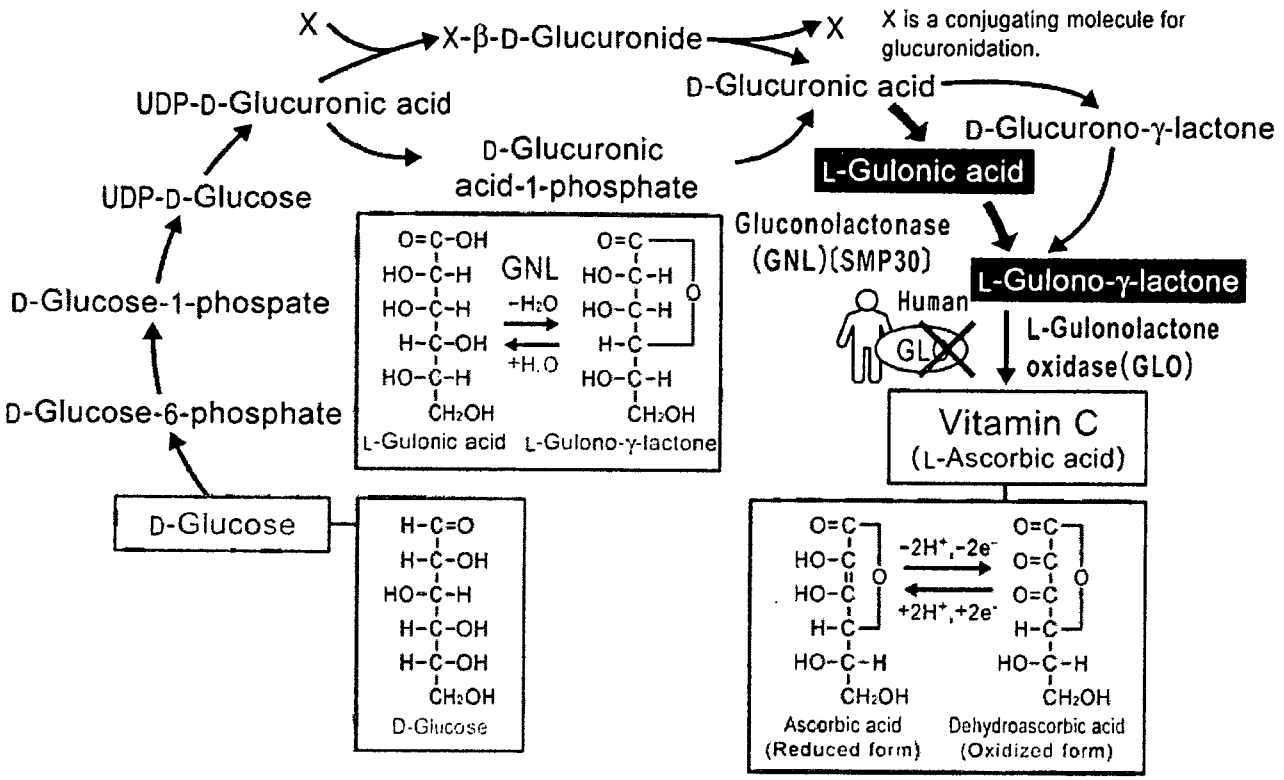

Figure 3 Vitamin C biosynthesis pathway. The pathway from D-glucose to L-gulonic acid is shared with that of early steps in the uronic acid cycle. X is a conjugating molecule for glucuronidation. SMP30 is a gluconolactonase (GNL), which catalyzes from L-gulonic acid to L-gulono-γ-lactone. In humans, L-gulonolactone oxidase (GLO) is absent because of mutation.

The lactonase reaction with L-gulono-γ-lactone is the penultimate step in vitamin C (L-ascorbic acid) biosynthesis (Fig. 3). SMP30-knockout mice fed a vitamin C-deficient diet did not thrive. They displayed symptoms of scurvy such as bone fracture and rachitic rosary and then died by 135 days after starting this vitamin C-deficient diet. The vitamin C levels in their livers and kidneys at the time of death were less than 1.6% of those in wild-type control mice. In addition, by using SMP30-knockout mice, we demonstrated that the alternative pathway of vitamin C synthesis involving D-glucurono-γ-lactone operates *in vivo*, although its flux is fairly small.

Additional and unique functions of SMP30 have also been reported. In experiments with the aforementioned HepG2 (HepG2/SMP30) cells expressed large amounts of SMP30, we observed a slower rate and decreased amount of DNA synthesis than in control HepG2 cells (mock transfected with pcDNA3 vector only).

Ultrastructural studies by scanning electron microscopy revealed numerous microvilli covering the surfaces of HepG2/SMP30 cells, whereas few microvilli appeared on control HepG2 cells.[22] Subsequently, transmission electron microscopy disclosed groups of HepG2/SMP30 cells with bile canaliculi and specialized adhesion contacts, such as tight junctions and desmosomes, at interplasmic membranes. However, in controls, units of only two cells were seen, and these lacked specialized adhesion junctions. Moesin,[23] which plays a crucial role in the formation of microvilli structures, and ZO-1,[24] which concentrated in tight junctions and adherence junctions located at the apical end of epithelial cells, are known to be concentrated in microvilli and at tight junctions, respectively. The intensity of moesin and ZO-1 staining in the contact regions of each cell was markedly higher in HepG2/SMP30 than in control cells. Moreover, moesin stained more interior areas, which corresponded to the microvilli of bile canaliculi. Clearly, bile canaliculi with microvilli formed at the apical ends of HepG2/SMP30 cells. These results indicate that SMP30 has an important physiological function as a participant in cell-to-cell interactions and imply that the downregulation of SMP30 during the aging process contributes to the deterioration of cellular interactivity.

Deficiency of SMP30

Originally, SMP30 was discovered because of its decrease with aging. If this decrease is long lasting, the deficiency of SMP30 in animal models can be regarded

as an ultimate decrease approaching zero. To elucidate the effect of this SMP30 decrease with aging, we introduced a null mutation of the *SMP30* gene into the germ line of mice.[25]

Despite the complete lack of SMP30, these mutant (SMP30-knockout) mice were indistinguishable from their wild-type littermates in terms of development and fertilization capability. We then investigated tissues' susceptibility for apoptosis induced by cytokines using primary cultured hepatocytes, because SMP30 could rescue cells from death caused by a calcium influx, using a calcium ionophore as previously described.[13,14] In SMP30-knockout mice, hepatocytes were more susceptible to apoptosis induced by tumor necrosis factor-α (TNF-α) plus actinomycin D (ActD) than hepatocytes from wild-type mice. In addition, the TNF-α/ActD-induced caspase-8 activity in hepatocytes from SMP30-knockout mice was twofold greater than that in matched cells from wild-type mice. In contrast, no significant difference was observed in the TNF-α/ActD-induced NFκB activation of hepatocytes from wild-type versus SMP30-knockout mice, indicating that SMP30 is not related to TNF-α/ActD-induced NFκB activation itself.

Moreover, deletion of the *SMP30* gene enhanced the susceptibility to another apoptosis inducer. After we treated SMP30-knockout mice with sub-lethal amounts of anti-Fas antibodies, liver injury was prominent in SMP30-knockout mice but not wild-type mice (Fig. 4).[25] Collectively, these results demonstrate that SMP30 acts to protect cells from apoptosis and other cell injuries.

Another molecular mechanism for the anti-apoptotic function of SMP30 was reported by our collaborators.[26] When cells were exposed to TNF-α plus ActD, cell viability was threefold higher in HepG2/SMP30 than control HepG2 cells. The presence of trifluoperazine, a calmodulin inhibitor, attenuated the anti-apoptotic effect of SMP30 in both cell types, but the effect was more prominent in HepG2/SMP30.

Western blot analyses revealed that Akt[27,28] as a survival factor was activated in HepG2/SMP30 cells in the presence or absence of TNF-α plus ActD. However, the activation was not observed in control HepG2 cells. Further, trifluoperazine inhibited Akt activation in HepG2/SMP30 cells. We therefore propose that interplay between calmodulin and SMP30 regulates Akt activity and, thus, that SMP30 acts as a survival factor in hepatocytes.

Next, we evaluated the effect of a SMP30 deficiency on life span.[29] SMP30-knockout mice are viable and fertile but lower in bodyweight and shorter in lifespan

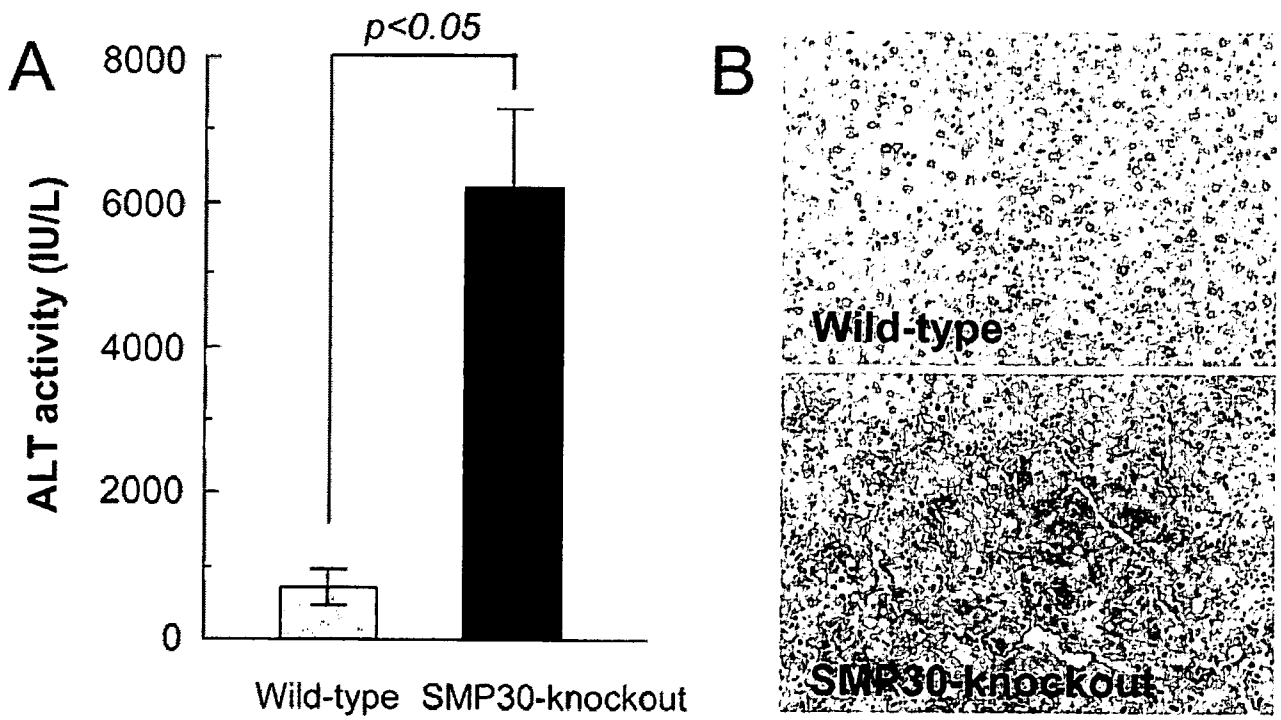

Figure 4 Anti-apoptotic activity of SMP30. Sub-lethal amounts of anti-Fas antibody were applied to SMP30-knockout and wild-type mice. (a) Serum alanine aminotransferase (ALT) levels of SMP30-knockout mice is higher than that of wild-type mice in peripheral blood after anti-Fas antibodies are applied. (b) Massive hemorrhage is visible in livers of SMP30-knockout mice but not wild-type mice.

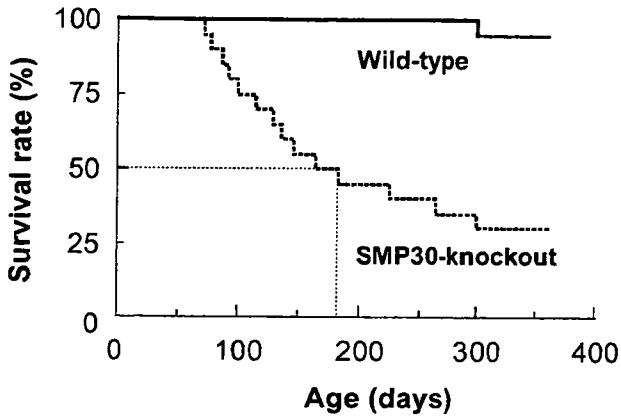

Figure 5 The lifespan is shortened in SMP30-knockout mice whose survival time was only 50%; that is, 180 days (6 months), in the 20 animals studied for comparison to the wild-type.

than their wild-type counterparts (Fig. 5). Histopathological examination showed no particular cause of the death in SMP30-knockout mice. The only noticeable event was marked emaciation in each individual. This finding suggests that the lack of SMP30 seems to be a model of "natural death." Because death often occurs in a background of malnutrition, the genuine cause deserves further study.

Via electron microscopy, hepatocytes from SMP30-knockout but not the wild-type mice at 12 months of age clearly contained many lipid droplets, abnormally enlarged mitochondria with indistinct cristae and enlarged lysosomes filled with electron-dense bodies. In liver specimens from SMP30-knockout mice, the marked number of lipid droplets visible around the central vein increased notably in size and amount as the animals aged. Biochemical analysis of neutral lipids, total hepatic triglycerides and cholesterol from SMP30-knockout mice showed approximately 3.6- and 3.3-fold higher levels, respectively, than those from age-matched wild-type mice. Moreover, values for total hepatic phospholipids from SMP30-knockout mice were approximately 3.7-fold higher than those for their wild-type counterparts.

By thin-layer chromatography analysis, phosphatidylethanolamine, cardiolipin, phosphatidylcholine, phosphatidylserine and sphingomyelin accumulations were detected in lipid extracts from the livers of SMP30-knockout mice. Conceivably, this abnormal lipid metabolism might be one cause of the shortened lifespan of these mice without SMP30.

Because SMP30 is expressed in almost all organs except those with hematopoietic function, we widened our search for the pathological features of aging beyond those in the liver and kidneys. As we previously reported, SMP30-knockout mice are novel models of senile lungs with age-related airspace enlargement and enhanced susceptibility to harmful stimuli.[30] Aging and smoking are considered as major contributing factors for the development of pulmonary emphysema. For that reason, we evaluated whether SMP30-knockout mice are susceptible to oxidative stress associated with aging and smoking.[31] In the lungs of SMP30-knockout mice, protein carbonyls tended to increase with aging and were significantly higher than in the age-matched wild-type mice. Exposure to cigarette smoke generated marked airspace enlargement with significant parenchymal destruction in the SMP30-knockout mice than in the wild-type mice. The protein carbonyls, malondialdehyde, total glutathione and apoptosis of lung cells were significantly increased after an 8-week exposure to cigarette smoke in the SMP30-knockout mice. Because our results suggest that SMP30 protects the lungs from oxidative stress associated with aging and smoking, the SMP30-knockout mouse could be a useful animal model for investigating age-related lung diseases such as emphysema.

In submandibular glands, the influence of a SMP30 deficiency is more intense than in other organs. For example, marked swelling of mitochondria and decreased numbers of secretory granules can be observed in 12-month old SMP30-knockout mice (Fig. 6).[32]

The expression of SMP30 in the brain has been detected, although at a very low level. Nevertheless, the effect of this deficiency is prominent.[33] We showed that the generation of reactive oxygen species (ROS) and nicotinamide adenine dinucleotide phosphate (NADPH) oxidase activities were significantly elevated in the brains of SMP30-knockout mice. The increased oxidative status in these mice was further confirmed by their increases of oxidatively modified proteins such as dityrosine formation and carbonylation in the cerebral cortex. Moreover, the brains of SMP30-knockout mice manifested increased amounts of Mac-1,[34] which is regarded as the key mediator responsible for the migration of neutrophil, protein and myeloperoxidase activity, supporting the putative anti-oxidative action of SMP30. Interestingly, the activities of other major anti-oxidant enzymes (i.e. superoxide dismutase, catalase and glutathione peroxidase) in the brain were not affected by SMP30 depletion. Our results documented that, in the brain, SMP30 has a protective action against oxidative damage without influencing anti-oxidant enzyme status.

Two morphological features considered to be a hallmark of senescence are apparent in SMP30-knockout mice. At 12-months of age, SMP30-knockout mice had clearly visible deposits of lipofuscin and senescent-associated β-galactosidase in their renal tubular epithelia.[35] These features are compatible with high electron dense deposits in lysosomes. This observation supports

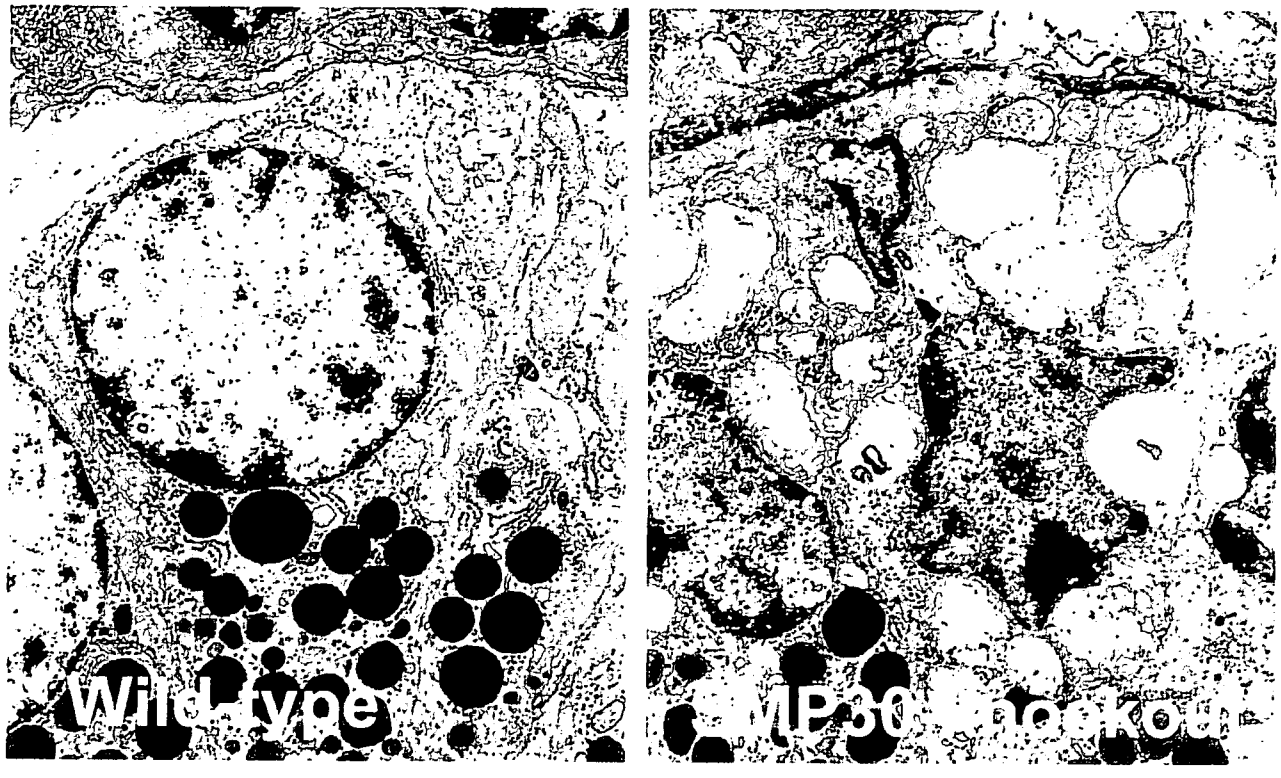

Figure 6 Degenerative subcellular components in SMP30-knockout mice. Granular duct cells of submandibular glands from a 37-week old SMP30-knockout mouse shows swollen mitochondria and a decrease of secretory granules.

the conclusion that the SMP30-knockout mouse is a useful model of ordinal senescence.

Most importantly, we have now identified an indisputable function of SMP30, that is, the production of vitamin C.[20] Because vitamin C is uniformly regarded as an anti-oxidant, we and others believe that a shortage of vitamin C induces senescence. This assumption has been proved by our observation that the lifespan of SMP30-knockout mice is significantly shorter than that of matched wild-type mice (Fig. 5).[29]

Modulation of SMP30

The suppressive effect of SMP30 on senescence has been introduced in this review. The other side of that coin is also true; enhancement of SMP30 expression prevents the pleiotropic dysfunction of organs during the aging process. Based on our studies, one can conclude that, in this context, the most influential factor causing senescence is oxidative stress. The relationship between SMP30 expression and oxidative stress is critical for understanding the mechanisms of senescence.

We used calorie restriction to explore age-related changes in *SMP30* gene expression.[36] The restriction of calories is the most probable paradigm for manipulating the development of senescence in humans.[37] The thrust of our investigation was based on the ability of calorie restriction to defend against age-related oxidative stress and the inflammatory process. The rats used for these experiments were divided into two groups: those fed ad libitum and those given a 40% calorie restricted diet. As expected, the animals' SMP30 expression declined with age, but in the calorie restricted group, this decline was clearly blunted (Fig. 7). Our data showed that the downregulation of SMP30 was accompanied by an increased generation of ROS, the oxygen-reactive entity. Therefore, the potent anti-aging and anti-oxidative action of a low-calorie diet effectively suppressed the age-related downregulation of SMP30 by ROS reduction.

Because age-related changes in SMP30 expression can be modulated by anti-oxidative action, the modulation of *SMP30* gene expression was explored by: (i) anti-oxidative calorie restriction of rats; (ii) pro-inflammatory lipopolysaccharide (LPS) administration to aged rats; (iii) oxidative stress promoter, *tert*-butylhydroperoxide (t-BHP) injection of mice; and (iv) t-BHP-treatment of Ac2F cells, a normal rat liver cell line.[38] We focused on the binding activity of an unidentified transcription factor at two sites located in the SMP30 promoter region.[39] Our results showed, first, that a calorie-restricted diet prevented the age-related decrease in SMP30 expression. Second, the binding of